NASA TECHNICAL MEMORANDUM

NASA TM-75543

# ULTRAVIOLET PHOTOMETRY OF VENUS: SCATTERING LAYER ABOVE THE ABSORBING CLOUDS

L.V. Ksanfomaliti, Ye.V. Dedova, V.G. Zolotukhin, G.I. Krasovskiy and V.M. Filimonova



Translation of "Ul'trafioletovaya Fotometriya Venery: Rasseivayushchiy Sloy nad Pogloshchayushchimi Oblakami," Academy of Sciences USSR, Institute of Space Research, Moscow, Report PR-288, 1976, pp. 1-30


NATIONAL AERONAUTICS AND SPACE ADMINISTRATION
WASHINGTON, D.C. 20546 SEPTEMBER 1978

STANDARD TITLE PAGE

| 1. Report No. NASA TM-75543 | 2. Government Accession No. | 3. Recipient's Catalog No. |
|---|---|---|
| 4. Title and Subtitle ULTRAVIOLET PHOTOMETRY OF VENUS: SCATTERING LAYER ABOVE THE ABSORBING CLOUDS | | 5. Report Date September 1978<br>6. Performing Organization Code |
| 7. Author(s) L.V. Ksanfomaliti, Ye.V. Dedova, V.G. Zolotukhin, G.I. Krasovskiy, V.M. Filimonova, Institute of Space Research Academy of Sciences USSR, Moscow | | 8. Performing Organization Report No.<br>10. Work Unit No.<br>11. Contract or Grant No. NASw-3199 |
| 9. Performing Organization Name and Address Leo Kanner Associates Redwood City, California 94063 | | 13. Type of Report and Period Covered Translation |
| 12. Sponsoring Agency Name and Address National Aeronautics and Space Administration, Washington, D.C. 20546 | | 14. Sponsoring Agency Code |

15. Supplementary Notes

Translation of "Ul'trafioletovaya Fotometriya Venery: Rasseivayushchiy Sloy nad Pogloshchayushchimi Oblakami," Academy of Sciences USSR, Institute of Space Research, Moscow, Report PR-288, 1976, pp. 1-30.

16. Abstract Experimental measurements by ultraviolet photometers aboard Venera-9 and -10 are presented, discussed and compared with various theoretical models of the ultraviolet structure of the atmosphere of Venus. The model in best agreement with observation provides for a finely dispersed, 8 km thick Rayleigh scattering layer above the primary cloud cover. Dark contrast details are considered to be breaks or areas of lower optical thickness in the upper scattering layer.

| 17. Key Words (Selected by Author(s)) | 18. Distribution Statement Unclassified-Unlimited | | |
|---|---|---|---|
| 19. Security Classif. (of this report) Unclassified | 20. Security Classif. (of this page) Unclassified | 21. No. of Pages | 22. Price |

## ANNOTATION

The ultraviolet photometry carried from aboard Venera-9 and Venera-10 permits it to be stated that there is a finely dispersed medium of irregular altitude, about 8 km thick, with nearly Rayleigh scattering, above the surface of the primary cloud layer. Comparison of experimental and calculated data gives satisfactory agreement, for an optical thickness of the scattering medium of 0.6-0.9. A single scattering albedo of no more than 0.994 was obtained for the primary cloud layer.

It was shown that dark contrast details can be considered as breaks or a decrease in optical thickness in the upper scattering layer. This explains the nature of the ultraviolet images of Venus. The upper boundary of the scattering layer is at an altitude of 76 km above the surface of the planet.

# ULTRAVIOLET PHOTOMETRY OF VENUS: SCATTERING LAYER ABOVE THE ABSORBING CLOUDS

L.V. Ksanfomaliti, Ye.V. Dedova, V.G. Zolotukhin, G.I. Krasovskiy and V.M. Filimonova, Institute of Space Research, Academy of Sciences USSR, Moscow

The nature and structure of the atmosphere of Venus remained /3* unknown for a long time. Significant progress has been achieved only in recent years, with the use of spacecraft. Seven vehicles of the Venera series and two Mariners, launched beginning in 1967, have shown that the atmosphere of this planet is very unlike the atmosphere of the Earth. Studies in the ultraviolet range, where unique details are observed on the surface of the cloud layer, are of particular interest. Photometric measurements, carried out from aboard the Venera-9 and Venera-10 artificial satellites, first permitted a detailed study of the brightness distribution over the disc of the planet. Numerous measurements have been carried out at various phase angles of the planet, with high spatial resolution, in the 3300 to 8000 A range.

The basic task of ultraviolet photometry is study of the light scattering relationships in the cloud and, to some extent, above the clouds layers of the atmosphere, contrast measurement, study of the structure of the upper part of the cloud layer and the nature of the dark and light formations.

The photometric measurements were carried out by means of three instruments installed aboard each vehicle. The basic one is a photometer with the following parameters: wavelength at the transmission maximum of the interference filter is 3520 A

*Numbers in the margin indicate pagination in the foreign text.

(Venera-9) and 3450 A (Venera-10), the transmission band at the 0.5 level is 180 and 170 A, respectively. The field of view /4
pattern width of the instrument at the 0.5 level is 16" (0.0047 radian). The statistical error of measurement is not over 0.4%. However, the absolute calibration error is considerably higher. The axis of the instrument is parallel to the axis of the infrared radiometer, which permits combined analysis of the results. The other two instruments, multifilter photometer-polarimeters, have eight subranges from 3350 to 8000 A. The pattern width is 34' (0.01 radian). The measurement time in each of the filters is 1 sec. The optical axis of one instrument is parallel to the axis of the ultraviolet photometer, but the axis of the other is deployed at 36° in the direction of movement in the calculated orbital plane. This system permits measurements to be carried out simultaneously for two values of the phase angle $\phi$. The brightness scale of the photometer-polarimeter is logarithmic. Therefore, the smaller the measured value, the less the error. However, with average brightness values, the measurement accuracy is considerably lower than that of the ultraviolet photometer.

The target of the photometric measurements is the upper story of the cloud cover of Venus, the boundary of which is at altitude of 64-67 km [1], and the layer of the atmosphere located somewhat higher. The pressure at these altitudes is 15-100 mb and density, $(4-20)\cdot10^{-5}$ g/cm$^3$. The cloud layer aerosol is spherical particles with an average diameter of about 2 μm, which evidently consist of concentrated sulfuric acid [2]. It was shown by the Mariner-10 measurements that the cloud cover pattern in the ultraviolet is distinguished by significant irregularities.

The brightness curves along the orbit, obtained in the first days of operation of Venera-9 and Venera-10, confirmed the presence of considerable contrast at 3500 A (Fig. 1), which reached ±10% or more, with respect to the smoothed curve. On the average, this smoothing gives a result which is close to Lambert's law, a cosine curve of the zenith distance /5 of the sun $M_1$. At other wavelengths from 4000 to 8000 A, the nature of the change in brightness is very even.

In different measurements, ultraviolet profiles of several types form: smooth, with small details and with extended contrast details.

Curves for different wavelengths are shown in Fig. 2, at an arbitrary vertical scale (Venera-9, 28 October 1975). The phase angle was 57°. The Moscow time of measurements, $M_1$ and the cosine of the zenith distance of the vehicle $M_2$ are plotted on the abscissa. The orbital path is through the equatorial zone, in the latitude region from -15° to +39°. The vehicle moved from the night side to the day side. The sharp drop in the curves on the right side corresponds to descent of the optical axis of the instrument from the light limb of Venus. The nature of all the curves is similar.

However, in a number of cases, a UV profile with a sharp peak, which appears in the zone of the light limb, matches the smooth curves in the range from 4000 to 8000 agnstroms. We see such results in the same session of 26 October, at a larger phase angle (Fig. 3). Despite the insignificant difference in the 3500 and 4000 A wavelengths, there is no similarity between these profiles. On the other hand, the 7000 A curve practically coincides with the 4000 A curve. This can be

interpreted as an argument in favor of Rayleigh scattering of the ultraviolet in the medium with finely dispersed particles, due to a sharp increase in optical thickness of such a medium at the limb of the planet. In such a case, a model in which the photons of all wavelengths are scattered by the same medium [3] is not consistent with observations. An alternative model should contain a layer which scatters the ultraviolet, and which is above the basic absorbing medium. The scattering layer should have breaks, which also permit explanation of Fig. 2.

However, there is another possible cause. The sharp peak may be due to considerable actual absorption, which is especially noticeable at small values of $M_2$. /6

In order to chose between these two possibilities, we attempted to find a calculated profile, which would closely correspond to the experimental results. Among the latter, a UV brightness curve was selected, which was obtained by Venera-9 on 13 November 1975, at a phase angle of 122°. There are practically no details in it, which makes the comparison easier.

First of all, as a very rough approximation, a profile was calculated for isotropically scattering and absorbing particles, with the use of the Chandrasekar [4] and Sobolev [5] N functions. In this case, the calculated brightness profile has the following form:

$$B = \mu_1 F \tilde{\omega}_0 \frac{H(\mu_1)\cdot H(\mu_2)}{4(\mu_1+\mu_2)}, \qquad (1)$$

where $\tilde{\omega}_0$ is the single scattering albedo with a spherical indicatrix and F is the flux. The actual asphericity of the

indicatrix was taken into account by calculation of the actual single scattering albedo a:

$$a = 1 - (1 - \tilde{\omega}_0)\cdot\left(1 - \frac{X_1}{3}\right), \qquad (2)$$

where $X_1$ is the first coefficient of expansion of the indicatrix in Legendre polynomials. According to ground based observations of Venus, $X_1=2.3$ in the UV range. This corresponds to considerable forward elongation of the indicatrix.

Together with the experimental data, three curves (1) are shown in Fig. 4, for $\tilde{\omega}_0$ 1.0, 0.975 and 0.8 (a is 1.0, 0.994 and 0.953, respectively). It is evident that the difference between calculation and experiment is considerable, even in the latter case, which corresponds to an impracticably low single scattering albedo. On the basis of the Wang approximation [6]

$$\frac{1+A_{sph}}{1-A_{sph}} = \left[\frac{(4-\tilde{\omega}_0)(3-\tilde{\omega}_0 X_1)}{12(1-\tilde{\omega}_0)}\right]^{1/2} \qquad (3)$$

the spherical albedo for $\tilde{\omega}_0=0.8$ is only 0.11, which is not confirmed by observation. According to the data of [7], ground based determinations for 3500 A give $A_{sph}=0.52$. /7

Thus, the experimental data fail to explain the large actual absorption, which cannot be attributed only to incorrectness of the approximate solution using the N functions. The fact is that, among the experimental material, curves can be found, which quite well approximate the solutions with the N functions. The upper part of Fig. 5 is an example, where the brightness curve obtained by Venera-9 on 9 November 1975 is fairly close to the experimental curve, at a=0.993. This corresponds to $A_{sph}=0.45$. There is an

appreciable deviation only in the zone of the limb, in which these discrepancies are actual: the spatial resolution of the photometer at this point corresponds to a 0.4 minute interval on the horizontal scale (if the resolution is considered as the time of passage of a point of the cloud cover surface by the pattern, with allowance for the slant range and velocity components perpendicular to the optical axis). The divergence in the lower part of the curve of Fig. 5 is more significant. On the other hand, the large differences between the calculated and experimental curves are especially well illustrated by Fig. 6, where the brightness variations in the Venera-9 measurements of 28 October 1975 and the curves for a=0.994, 0.982 and 0.953 are presented.

The results obtained for a two layer model are very much better in line with experiment. It is assumed that there is Rayleigh scattering in the upper layer, and that considerable actual absorption occurs in the primary cloud layer. A serious argument in favor of Rayleigh scattering is the sharp decrease in contrast at 4000 A. This is easily explained by a decrease in the contribution of scattering in the upper layer (as $\lambda^{-4}$). The upper layer should be of variable thickness /8 and have a considerable number of breaks (or sections of reduced optical thickness), through which the lower layer is observed. The contrasts between the dark and light details also are evidence in favor of such a model. The average contrasts in Fig. 1 are ±8-10%. They reach ±17.5% in some measurements. With an average spherical albedo $A_{sph}$=0.52, this gives the values of $A_{sph}$ and a summarized in Table 1.

The minimum values of á in Table 1 are close to unity. If it is considered that the optical thickness of the upper

TABLE 1

| a Контрасты | ±8 | | ±10 | | ±12 | | ±17,5 | |
|---|---|---|---|---|---|---|---|---|
| | b Макс. | c Мин. | b Макс. | Мин.c | Макс.b | Мин.c | Макс.b | Мин.c |
| d $A_{сф}$ | 0,562 | 0,478 | 0,572 | 0,468 | 0,582 | 0,458 | 0,611 | 0,429 |
| e $\varpi_0(3)$ | 0,985 | 0,976 | 0,986 | 0,975 | 0,987 | 0,973 | 0,990 | 0,969 |
| f $a_{\Sigma}(2)$ | 0,997 | 0,994 | 0,997 | 0,994 | 0,997 | 0,994 | 0,998 | 0,976 |

[Translator's note: commas in tabulated figures are equivalent to decimal points.]

Key: a. Contrast %
b. Max.
c. Min
d. Asph
e. $\varpi_0$ from (3)
f a from (2)

layer of clouds is small (as is shown below, about 0.6-0.9), the probable value of the single scattering albedo for the upper layer alone will correspond to conservative scattering. On the other hand, the minimum values of a evidently concern the lower layer. The very low value a=0.976 most likely corresponds to some inhomogeneity.

A diagram of such a structure of the upper part of the cloud layer is shown in Fig. 7. The figure concerns only the day side of the planet. The altitude of the upper boundary of the primary cloud layer of 67 km has been adopted, in accordance with works [1] and [8]. The upper layer directly adjoins the basic layer, and it ends around an altitude of 75-76 km, more precisely, 8-9 km above the basic layer top. Estimates of the altitude difference are based on the Venera-9

and Venera-10 measurements in the area of the terminator (Fig. 8). While the brightness at all wavelengths drops rapidly beyond the terminator, at 3500 A, the illuminated area is traced much further, to a sun angle $\delta=3°$ below the horizon. Besides, the brightness apparently is too high for it to explain the twilight phenomena in the basic layer, where the actual absorption is high. This permits it to be proposed that we observe scattering in the upper layer. The brightness decreases linearly from the terminator to a point 320 km distant, where it turns out to be beyond the limits of sensitivity of the photometer. Its spatial resolution, recalculated to a time scale, is about 6 sec. On the assumption that the brightness of this zone is determined by single scattering, from elementary geometrical considerations, the altitude of the layer h can be estimated as

/9

$$h = R(\sec\delta - 1), \qquad (4)$$

which gives 8.4 km (here, R is the radius of Venus to the cloud layer).

The absence of a gap between the basic and upper layers was concluded, on the basis of the linear decrease in brightness beyond the terminator. It is easy to see that, in the case of a thin layer, the brightness curve in Fig. 8 would have a different form.

Brightness measurements in the zone of the terminator permit, with the remarks made above taken into account, the bulk scattering coefficient in the ultraviolet to be found. An estimate, which will be refined later, is $3.7\cdot10^{-6}$ $cm^{-1}$.

The resulting altitude of the scattering layer does not confirm former assumptions, based on some Mariner-10 photographs (85 km).

Some other remarks on Fig. 7. The inner boundaries of the day cloud layer, found in the works of Moroz et al [9] 49 and 32 km, and Marov et al [10], 57, 49 and 18 km, also are shown here. It is not excluded that an attempt to show all these data on a general diagram is premature. In any case, /10 the 67-49 km altitude of the lower boundary of the layer is consistent in both works. According to the data of [1], the cloud tops at night decrease to approximately 65 km. Of course, the location of the upper scattering layer in the night zone remains unknown.

The parameters of the two layer (relative to the ultra-voilet) scheme are based on some alternate versions of the calculation. The results were compared with the experimental data represented by the brightness curve in Fig. 4. It was assumed in all the alternate versions that the upper layer makes a contribution in the form of single scattering with a Rayleigh indicatrix (there is no actual absorption). This component, in accordance with [5], gives the brightness coefficient in the form

$$\rho(\mu_1, \mu_2, \varphi) = \frac{\chi_\rho(\gamma)}{4} \cdot \frac{1 - e^{-\tau_0(1/\mu_1 + 1/\mu_2)}}{\mu_1 + \mu_2} \qquad (5)$$

with an indicatrix

$$\chi_\rho(\gamma) = 3/4 \cdot (1 + \cos^2\gamma). \qquad (6)$$

Here, $\phi$ is the phase angle of the observed points (constant in each measurement) and $\gamma$ is the scattering angle

$$\gamma = \pi - \varphi \qquad (7)$$

In the first alternate version (the roughest among the two layer models), a model of the atmosphere of Mars was used [5], in which the brightness coefficient $\rho_n$ implied a plane albedo of the basic cloud layer independent of $M_1$ and $M_2$, and estimated from $A_{sph}$ as 0.477:

$$\rho(\mu_1,\mu_2,\varphi)=\frac{\chi_p(\gamma)}{4}\cdot\frac{1-e^{-\tau_0(1/\mu_1+1/\mu_2)}}{\mu_1+\mu_2}+\rho_n\cdot e^{-\tau_0(1/\mu_1+1/\mu_2)} \quad (8)$$

The value of $\tau_0$ was assumed to be from 0.05 to 0.90. The /11
calculated results (in the form of the normalized derivative of $\rho M_1$) show that, with $\tau_0=0.90$, the curve passes fairly close to the experimental profile (Fig. 9), in the upper part of it, in any case.

Somewhat better results are given by the second alternate version, in which the second part of equation (8) is replaced by allowance for scattering by aerosol particles [5], with a strongly elongated scattering indicatrix

$$\chi_a(\gamma)=1+X_1\cdot\cos\gamma \quad (9)$$

with $X_1=2.3$ (ground based determinations for 3500 A).

In this case, the brightness coefficient

$$\rho(\mu_1,\mu_2,\varphi)=\frac{1}{4(\mu_1+\mu_2)}\cdot\left\{\chi_p(\gamma)\cdot\left[1-e^{-\tau_0(1/\mu_1+1/\mu_2)}\right]+\chi_a(\gamma)\cdot e^{-\tau_0(1/\mu_1+1/\mu_2)}\right\}, \quad (10)$$

in which the single scattering albedo for the second term is assumed a=1. Normalized $\rho M_1$ for $\tau_0=0.1$, 0.4 and 0.8 are shown in Fig. 10. With increase in $\tau_0$ from 0.05 to 0.2, the upper parts of the calculated curves deviate to the left and the lower, to the right and vice versa further on. On the whole,

at $\tau_0=0.8$, the curve is somewhat closer to the experimental data than for the first version.

The most convincing coincidence with experiment was obtained in the third alternate version. It is assumed here that there are two types of scattering in the lower layer: conservative, with an elongated indicatrix (9), combined with isotropic, with single scattering albedo a from 1 to 0.953. Each of these parts was taken into account by coefficient $\beta<1$ and $1-\beta$, respectively:

$$\rho(\mu_1,\mu_2,\varphi)=\frac{1}{4(\mu_1+\mu_2)}\cdot\left\{\chi_\rho(\gamma)\cdot\left[1-e^{-\tau_0(1/\mu_1+1/\mu_2)}\right]+\right.$$
$$\left.+\beta\cdot\chi_\rho(\gamma)\cdot e^{-\tau_0(1/\mu_1+1/\mu_2)}+(1-\beta)\cdot\tilde{\omega}_0\cdot H(\mu_1)\cdot H(\mu_2)\cdot e^{-\tau_0(1/\mu_1+1/\mu_2)}\right\}. \quad (11)$$

This version was calculated for $\tau_0$ from 0.2 to 0.9 and $\beta$ from 0.1 to 0.8. Changes in location of the curves are monotonic. A family of normalized $\rho M_1$ curves is shown in Fig. 11, with a=0.994, $\tau_0=0.9$ and $\beta$ from 0.1 to 0.8. Their coincidence with the experimental profile is obvious. The calculated curves, obtained with large actual absorption (a=0.953), for $\tau_0=0.6$ (Fig. 12) and 0.9 (Fig. 13), also are close to it. However, the middle portion of the experimental profile is closer to the curve in Fig. 11. The results change little with substitution of $X_p(\gamma)$ for $X_a(\gamma)$. /12

The physical meaning of the last version is that the finely dispersed medium of the upper layer also penetrates into the basic cloud layer.

The lower portion of the experimental curve fails to be expressed by the calculated profile. An analysis shows that

the curve is asymmetrical relative to $M_1$ and $M_2$. It would appear that the most likely cause of this is a random inhomogeneity in the basic layer. But, the same deviation in the left portion can be seen in Figs. 2, 5 and 6. A possible explanation is connected with the two thermal emission regimens of Venus described in [1,8]. In precisely this zone near the evening terminator, where persistent "inhomogeneities" are observed, there is a transition region from the low daytime to the higher nighttime brightness temperatures in the thermal IR range. The connection of these two phenomena probably is not random. In this case, there should be a similar pattern in the morning terminator zone.

Thus, it can be stated that the structure of the upper layer of clouds of Venus evidently corresponds to the model adopted: a 8-9 km thick scattering layer is located directly above the upper boundary of the basic clouds. The layer has $\tau_0=0.6-0.9$ and a bulk scattering coefficient $\sigma\approx3.7\cdot10^{-6}$ cm$^{-1}$; it consists of finely dispersed particles, it has a flocculent structure, and it scatters the ultraviolet without appreciable /13
absorption. At the same time, the basic cloud layer strongly absorbs the ultraviolet. Such a structure easily explains the ultraviolet pattern of the basic layer. The dark bands form where the lower layer is seen through the reduced optical thickness of the upper. There are fewer of them than of the light sections, where $\tau_0$ reaches 2, and which form light cloud layers in perspective. The latter circumstance confirms that the scattering layer is located above the absorbing layer.

References


1. Ksanfomaliti, L.V., Ye.V. Dedova, L.F. Obukhova, V.M. Pokras, N.V. Temnaya and G.F. Filippov, Astr. zhurn. 4 (1976).

2. Young, A.T., Icarus 18, 564 (1973).

3. Young, A.T., in the collection The Atmosphere of Venus, NASA, Sp-382, 1975, p. 12.

4. Chandrasekar, S., Perenos luchistoy znergii [Radiant Energy Transport], Foreign Literature Publishing House, 1953.

5. Sobolev, V.V. Rasseyanie sveta v atmosferakh planet [Light Scattering in the Atmospheres of the Planets], Nauka Press, 1972.

6. Wang, L., Astrophys. J. 174, 671 (1972).

7. Bigourd, G., C. Devaux, M. Herman and J. Lenoble, Icarus 26 73 (1975).

8. Ksanfomaliti, L.V., Ye.V. Dedova, L.F. Obukhova, N.V. Temnaya and G.F. Filippov, K.I. XIV/5, (1976).

9. Moroz, V.I., N.A. Parfent'ev, N.F. San'ko, V.S. Zhegulev L.V. Zasova and Ye.A. Ustinov, K.I. XIV/5, (1976).

10. Marov, M.Ya., B.V. Byvshev, K.N. Manuylov, Yu.P. Baranov, I.S.Kuznetsov, V.N. Lebedev, A.V. Maksimov, G.K. Popandopulo, V.A. Razdolin, V.A. Sandimirov and A.M. Frolov, K.I. XIV/5, (1976).

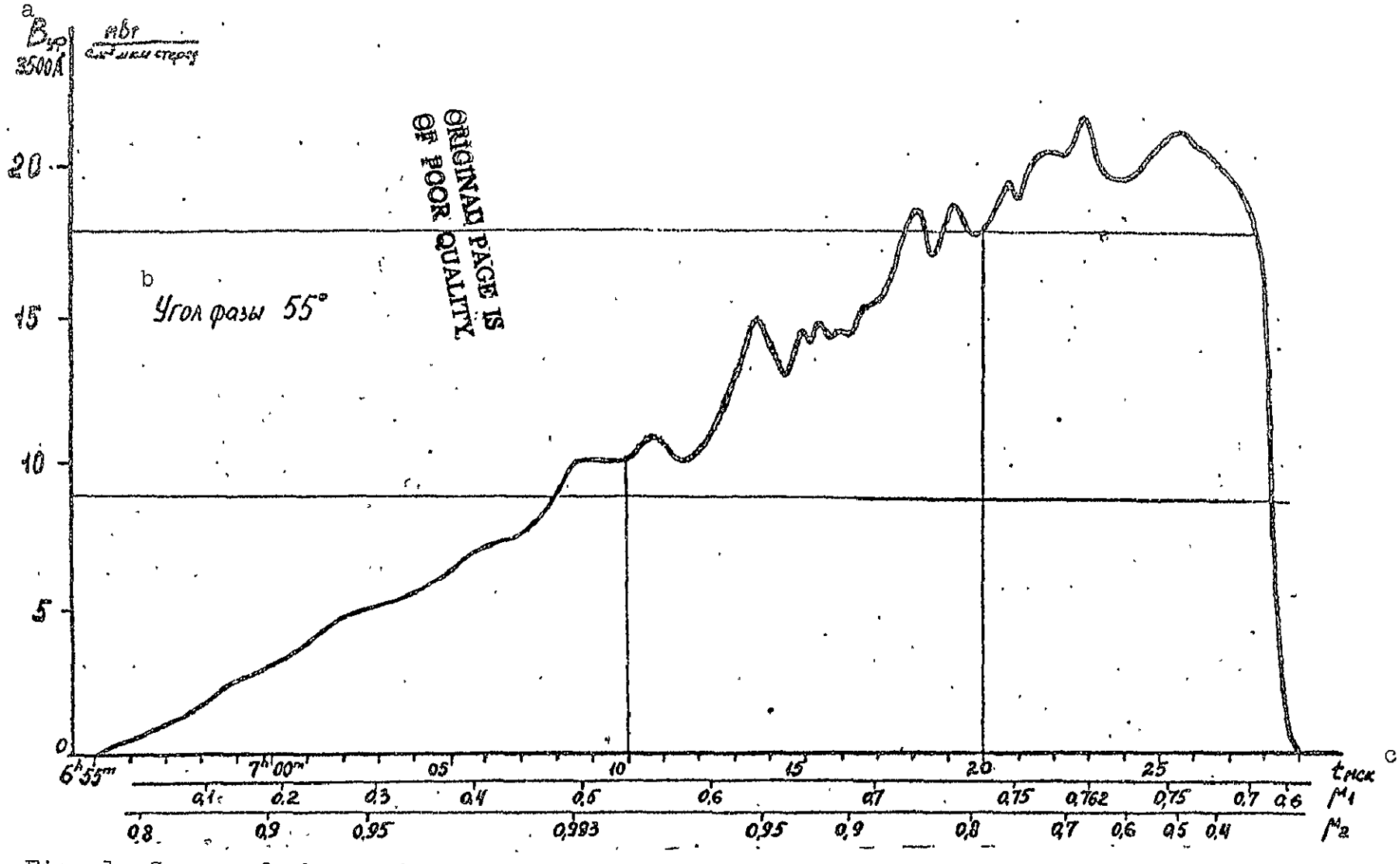


Fig. 1. Curve of change in brightness of cloud layer of Venus along Venera-9 orbit 26 October 1975; on abscissa, Moscow time of measurements, cosine of zenith distance of sun ($M_1$) and vehicle ($M_2$); ordinate in absolute brightness values.

Key: a. $V_{uv}$, $mW/cm^3 \cdot \mu m \cdot ster$ b. Phase angle c. $t_{Moscow}$

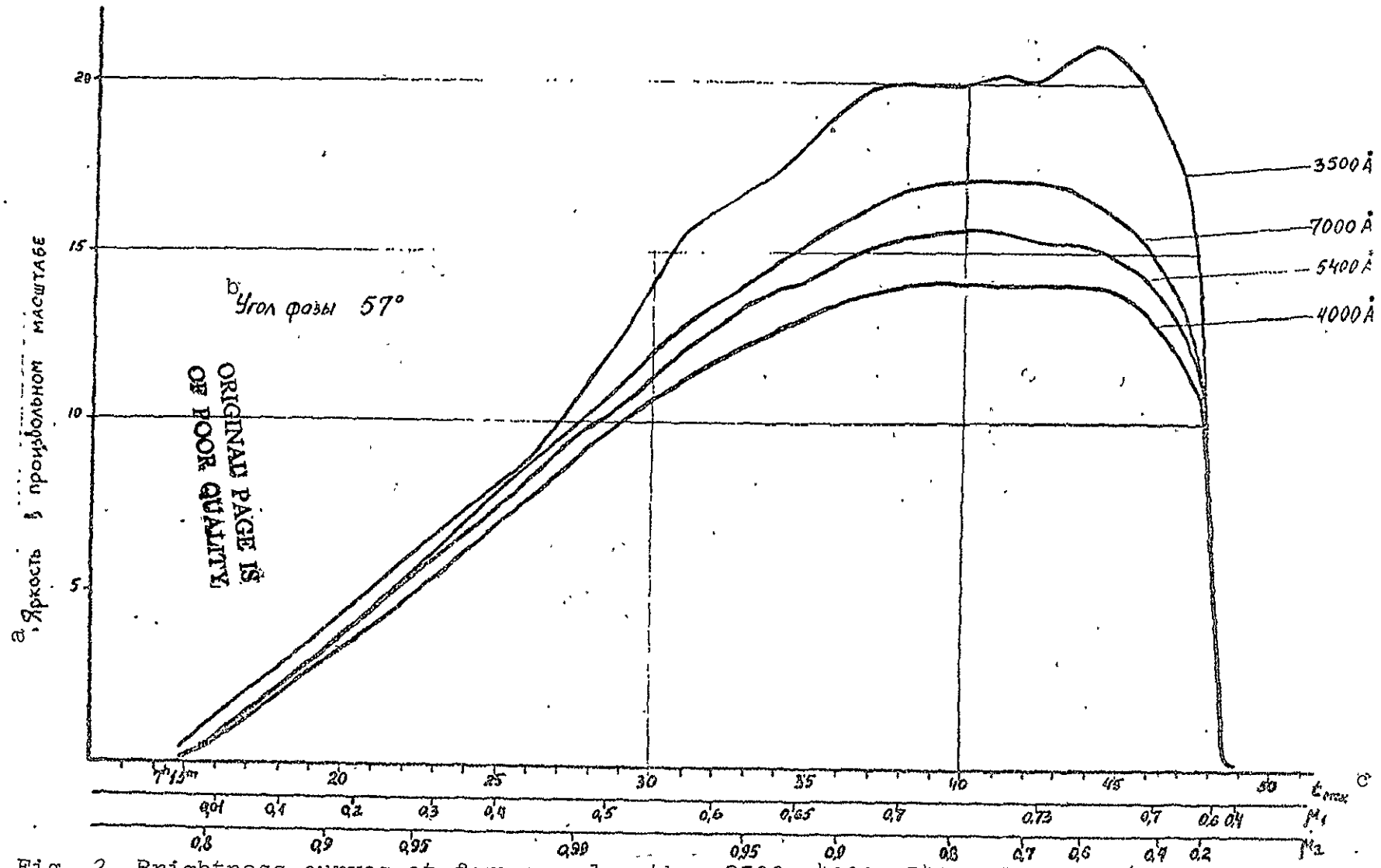


Fig. 2. Brightness curves at four wavelengths, 3500, 4000, 5400, 7000 A, from Venera-9 measurements 28 October 1975; abscissa same as in Fig. 1; ordinate, brightness in relative units; all curves have a similar nature.

Key: a. Brightness in relative units b,c. [same as in Fig. 1]

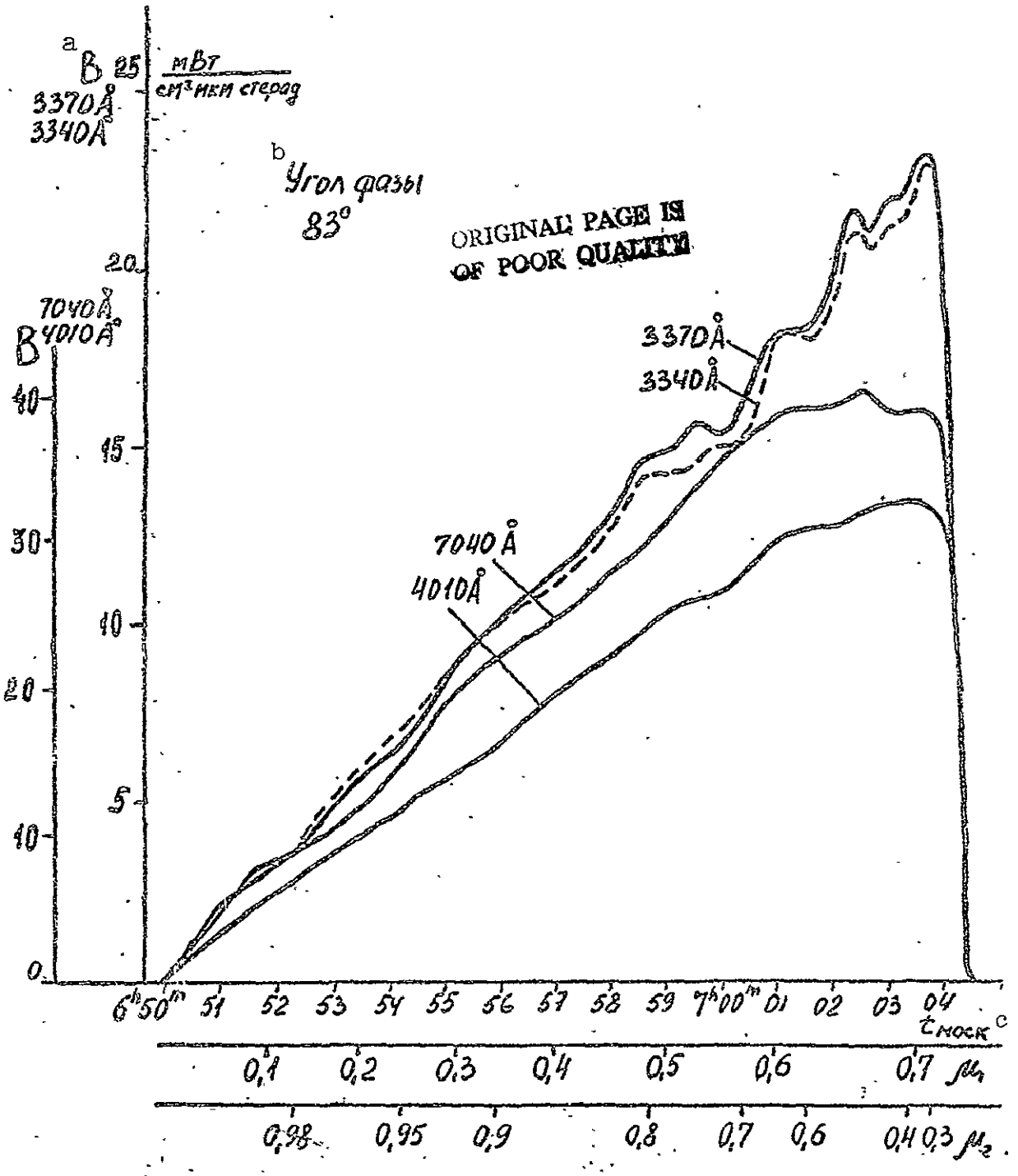


Fig. 3. Brightness curve along Venera-9 orbit 26 October 1975 at phase angle 83°; flight path close to Fig. 1 flight path; measurement error here larger than in Fig. 1, which is shown by superimposing two independently obtained curves for 3340 and 3370 A; 4010 A profile very similar to 7040 A profile, but unlike 3400 A profile.

[Key: same as in Fig. 1]

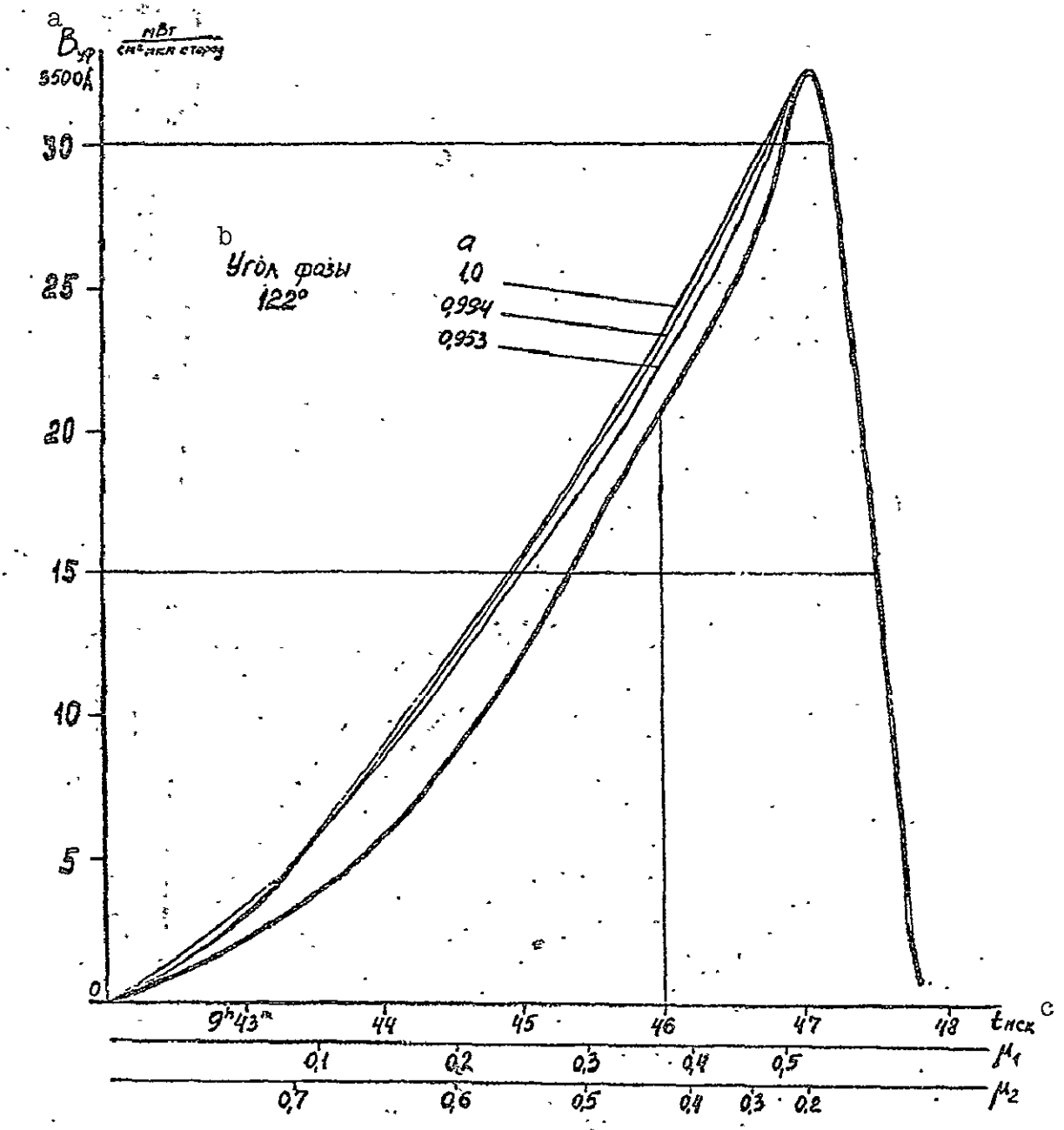


Fig. 4. Calculated curves for simplest case (1) at a=1, 0.994 and 0.953 and experimental data (Venera-9, 13 November 1975); phase angle 122°; brightness in absolute values; abscissa same as in Fig. 1.

[Key: same as in Fig. 1].

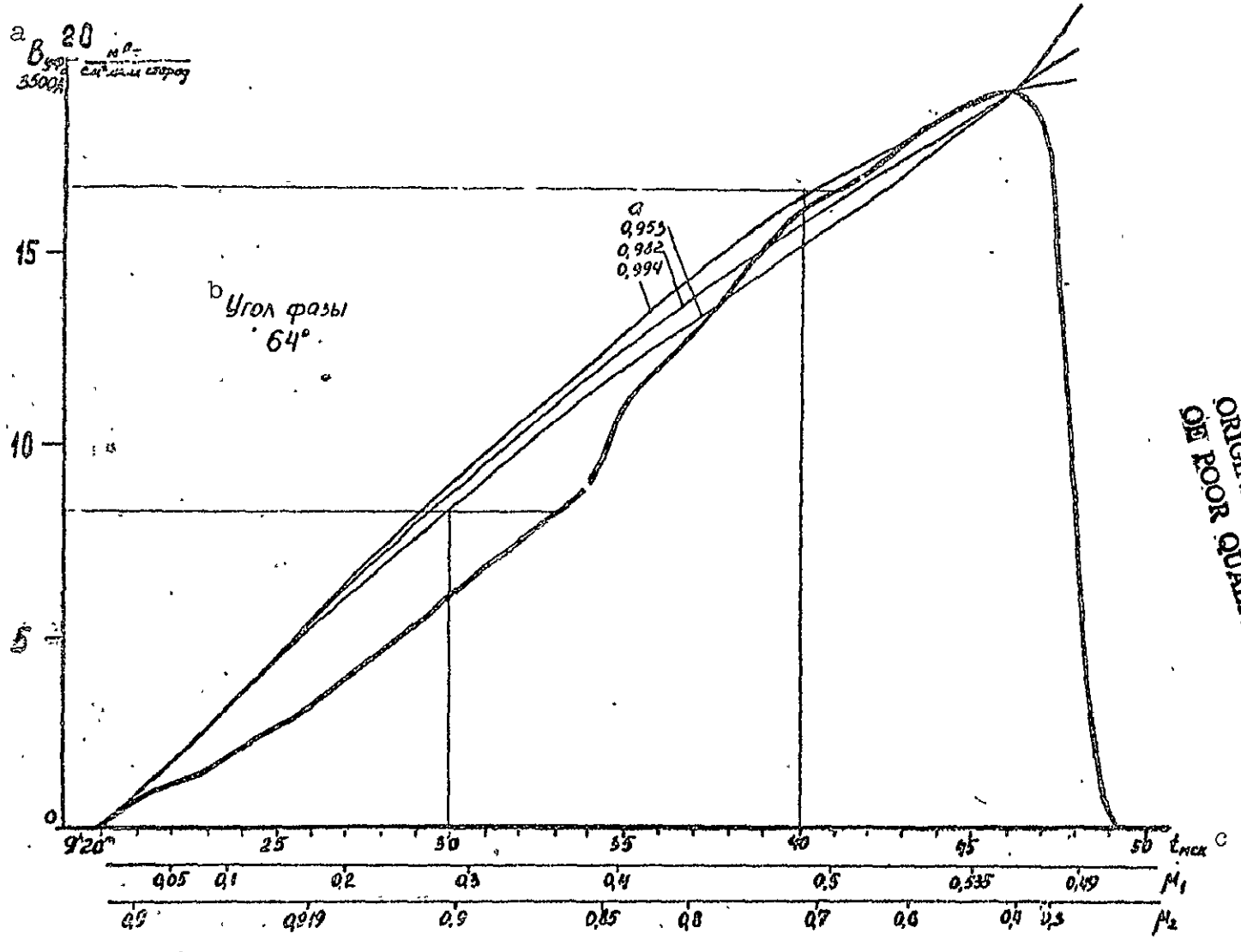




Fig. 5. Coincidence of upper part of experimental profile (Venera-9, 9 November 1975) with calculated for case (1), at a=0.993 and Asph= 0.45; phase angle 64°; brightness in absolute values.

[Key: same as in Fig. 1].

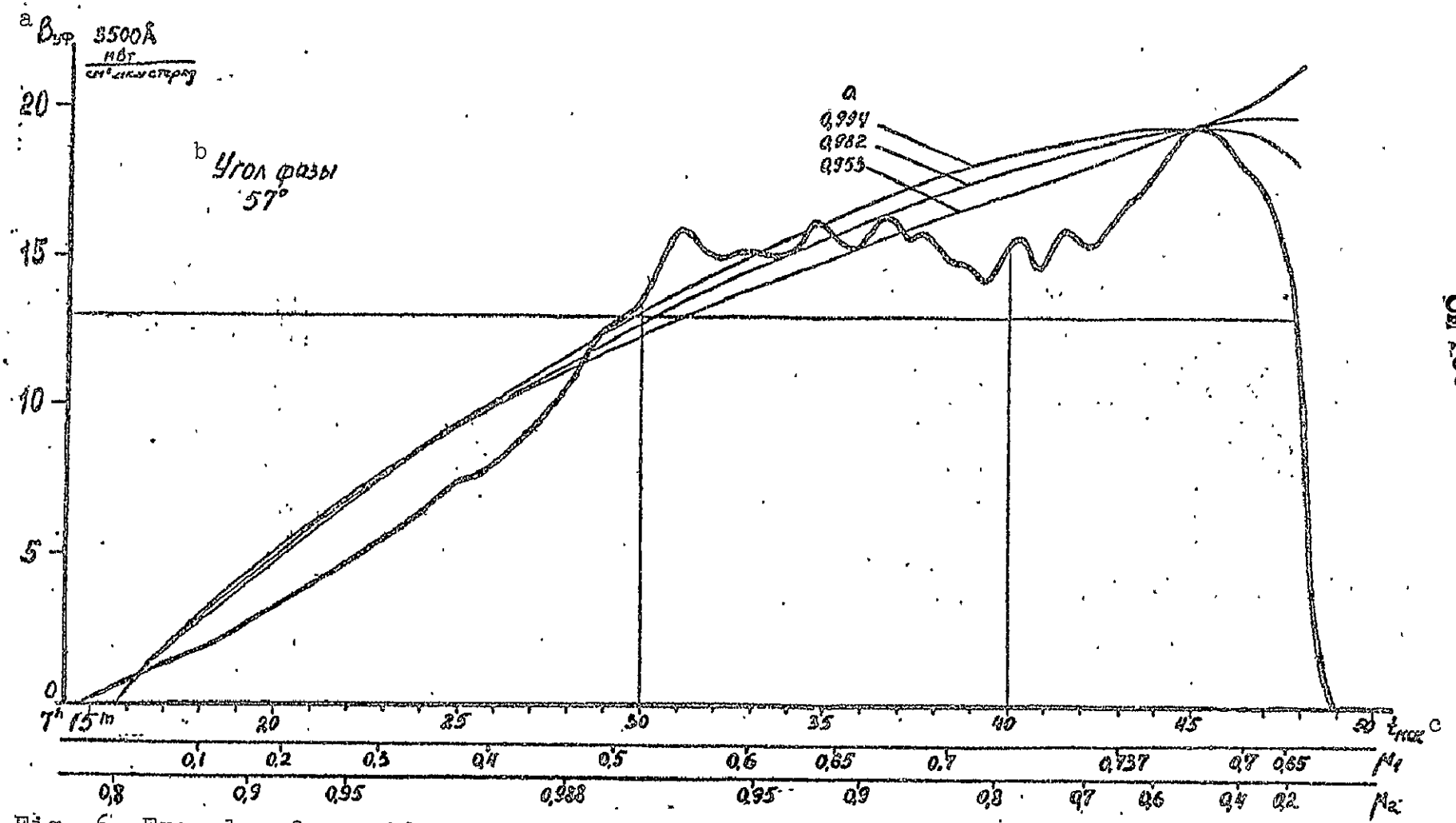


Fig. 6. Example of considerable disagreement between experimental and calculated brightness profiles (Venera-9, 28 October 1975); phase angle 57°.

[Key: same as in Fig. 1].

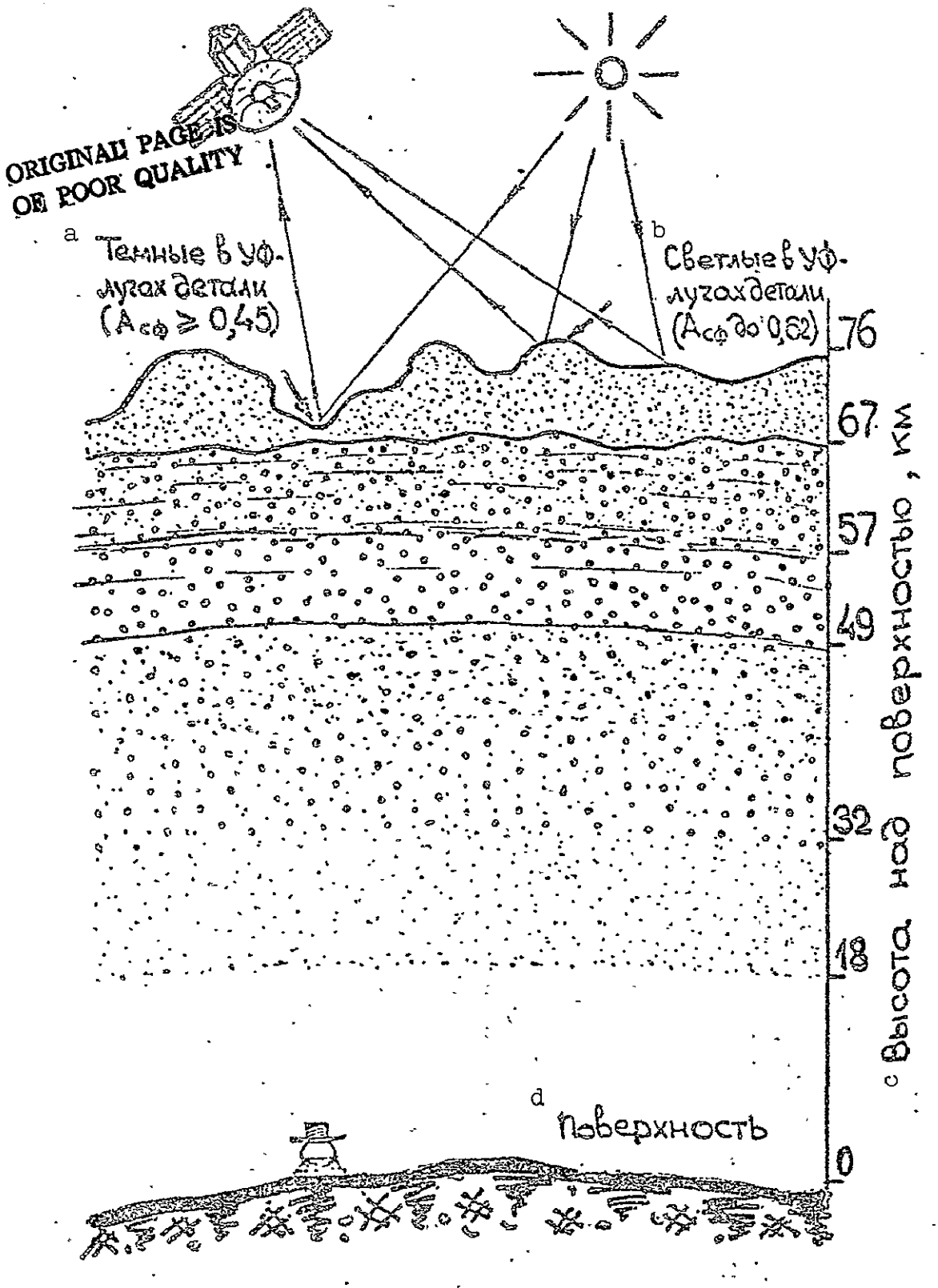


Fig. 7. Approximate diagram of Venus cloud cover structure; levels from 18 to 57 km taken from other works (references in text); diagram concerns only day side of planet; figure explains nature of dark and light details of ultraviolet image as difference in thickness of upper scattering layer with very small UV absorption; basic cloud cover, on the contrary, has considerable actual absorption, which produces characteristic banded structure.

Key: a. Dark UV details ($A_{sph} \geq 0,45$)

b. Light UV details ($A_{sph}$ up to 0.62)
c. Altitude above surface, km
d. Surface

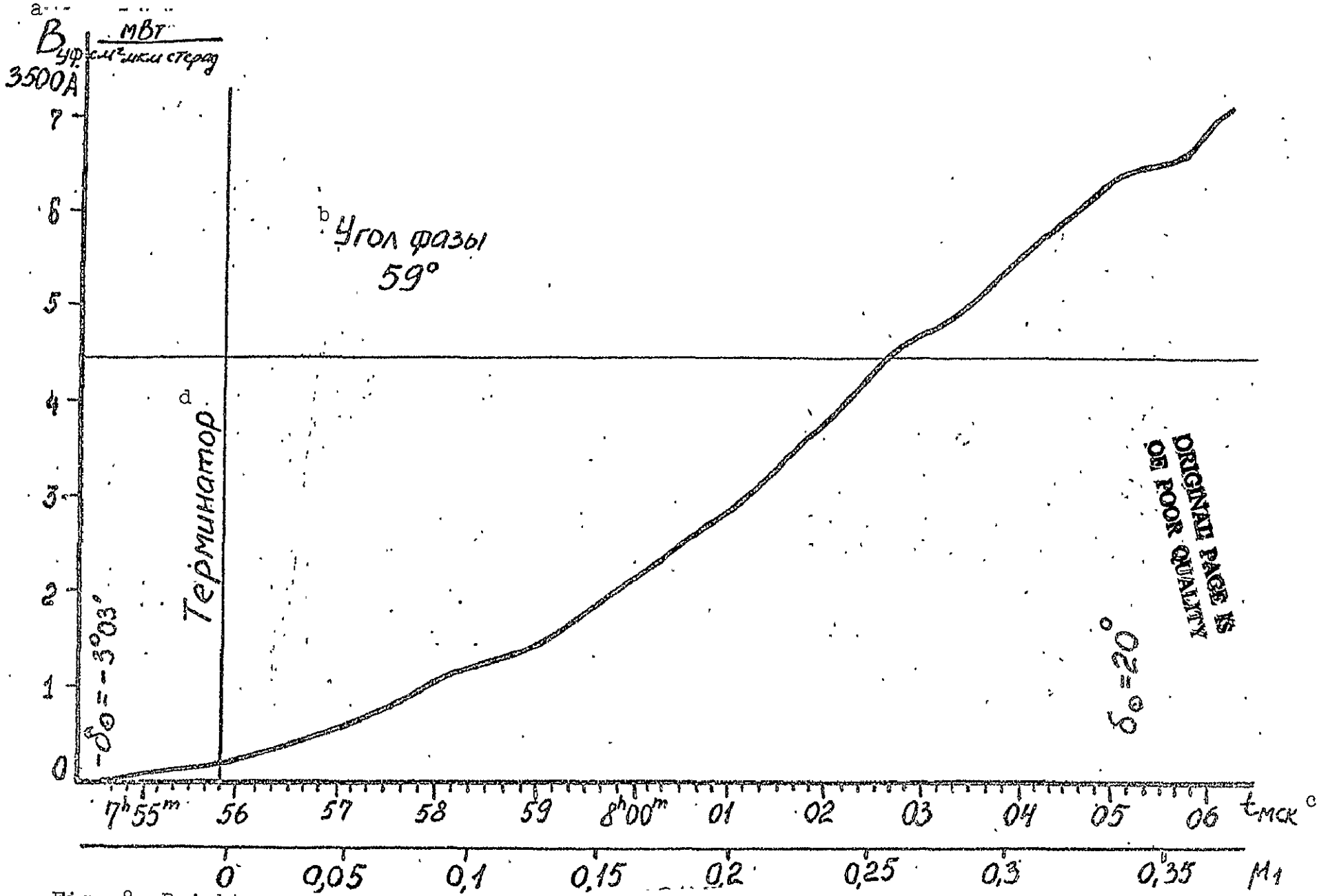


Fig. 8. Brightness variation in Venus evening terminator region at 3500 A; compared with 4000-8000 A range, illuminated zone is traced much further, up to sun angle 3° below horizon; great actual absorption in basic cloud layer permits proposal that light scattering in upper layer is observed beyond terminator; Venera-9, 1 November 1975.

Key: a-c. [same as in Fig. 1] d. Terminator

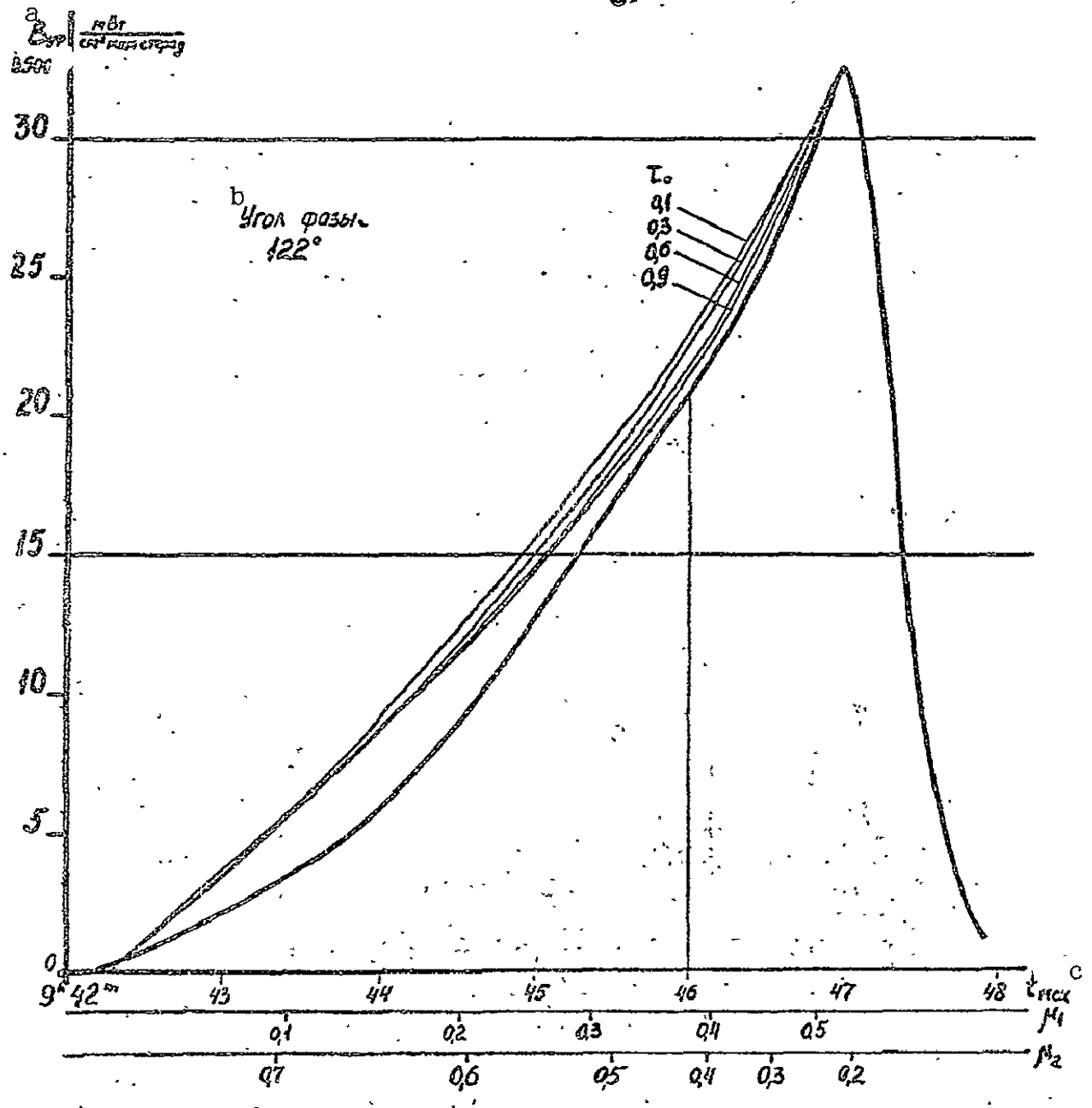


Fig. 9. Calculated curves for model with Rayleigh scattering in upper layer and brightness coefficient independent of $M_1$, $M_2$ in lower layer; experimental profiles same as in Fig. 4.

Key: [same as in Fig. 1].

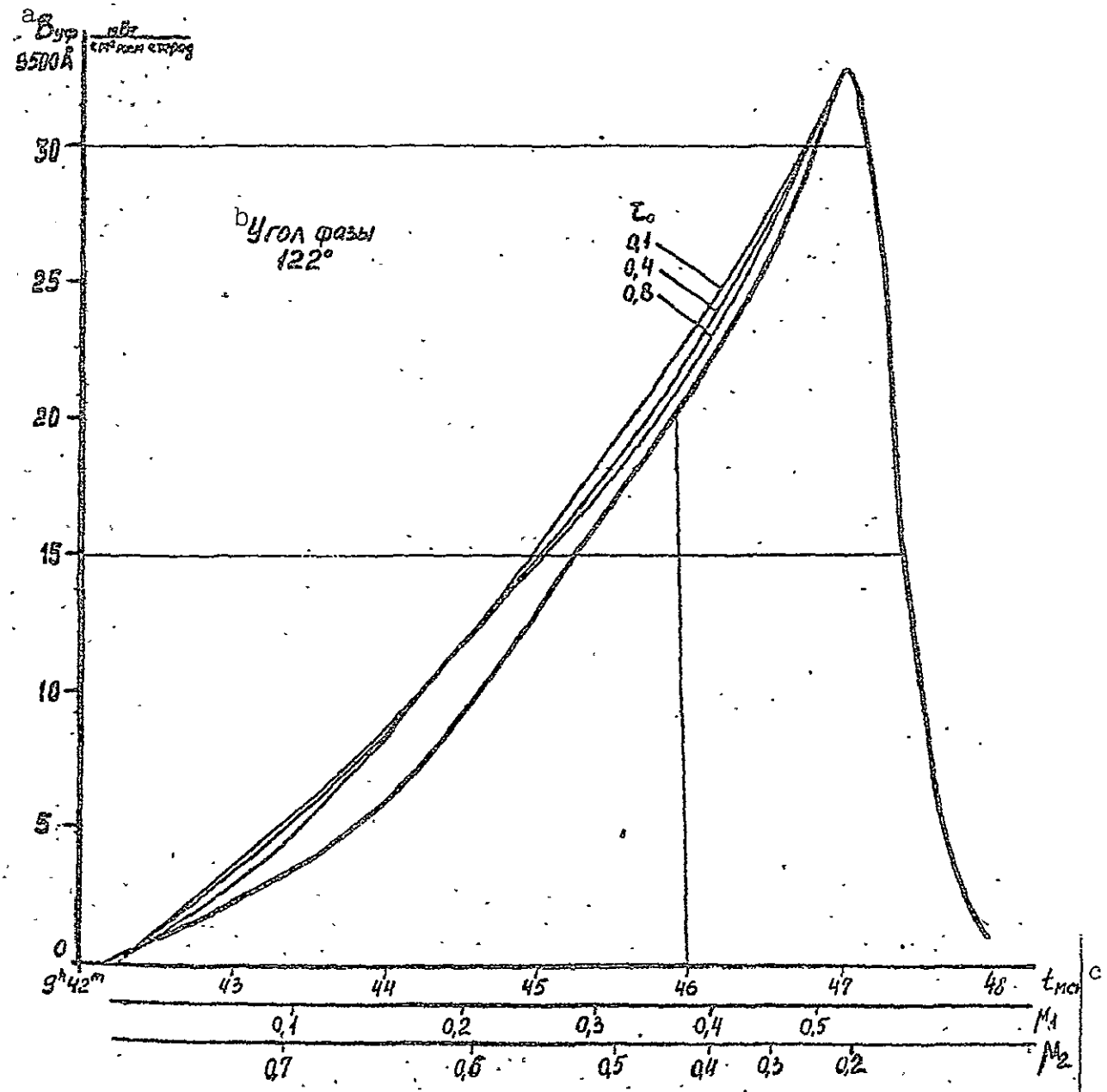


Fig. 10. Calculated curves for second alternate version: Rayleigh scattering in upper layer and strongly elongated indicatrix in lower layer at a=1; experimental profile same as in Fig. 4.

Key: [same as in Fig. 1]

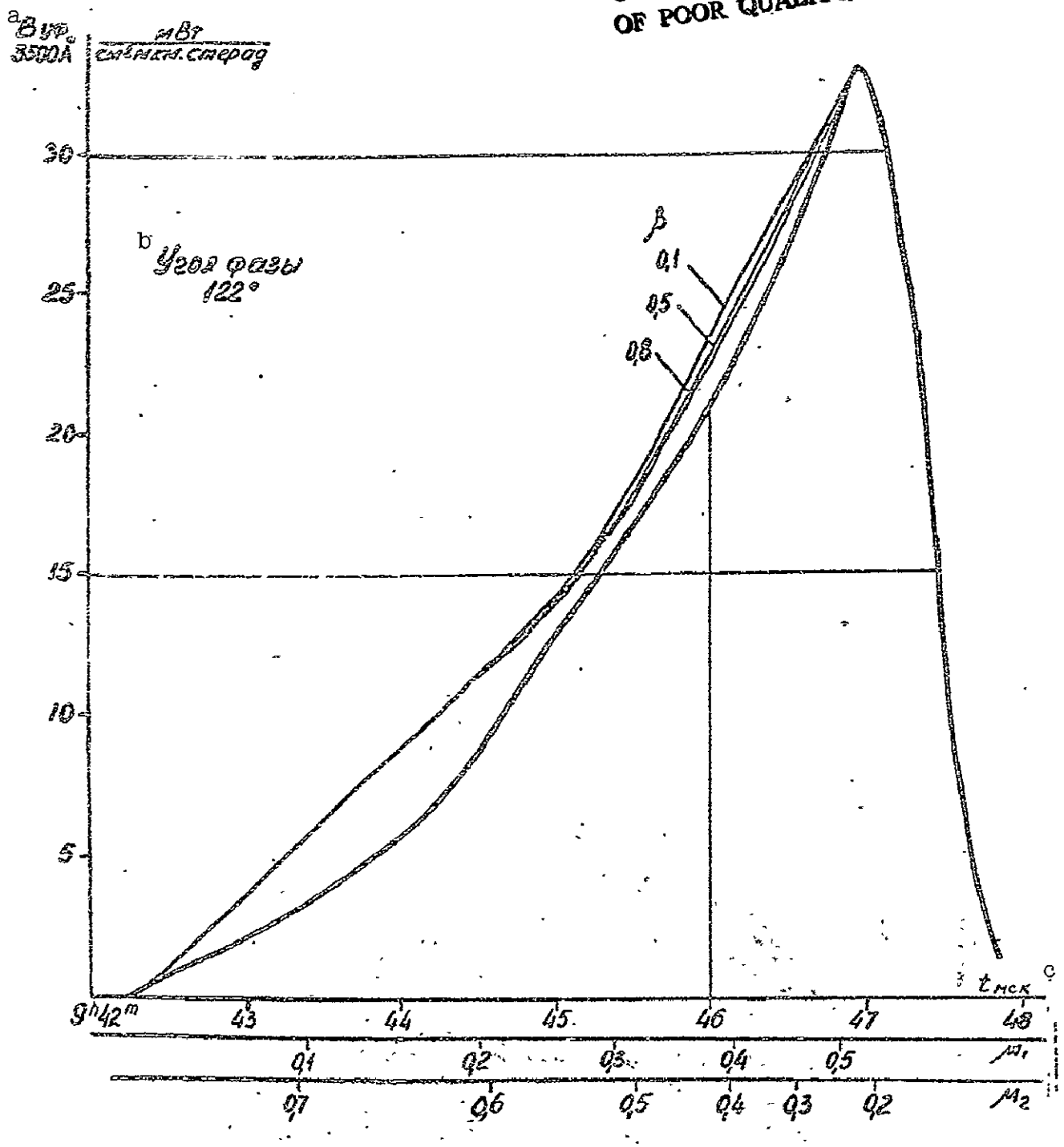


Fig. 11. Calculated curves for alternate version closest to experiment: upper layer, Rayleigh scattering; lower, combined isotropic scattering with actual absorption different from zero and conservative scattering with elongated indicatrix; contribution of first part (1-β), second, β; single scattering albedo a=0.994; optical thickness of upper layer $\tau_0$=0.9.

Key: [same as in Fig. 1].

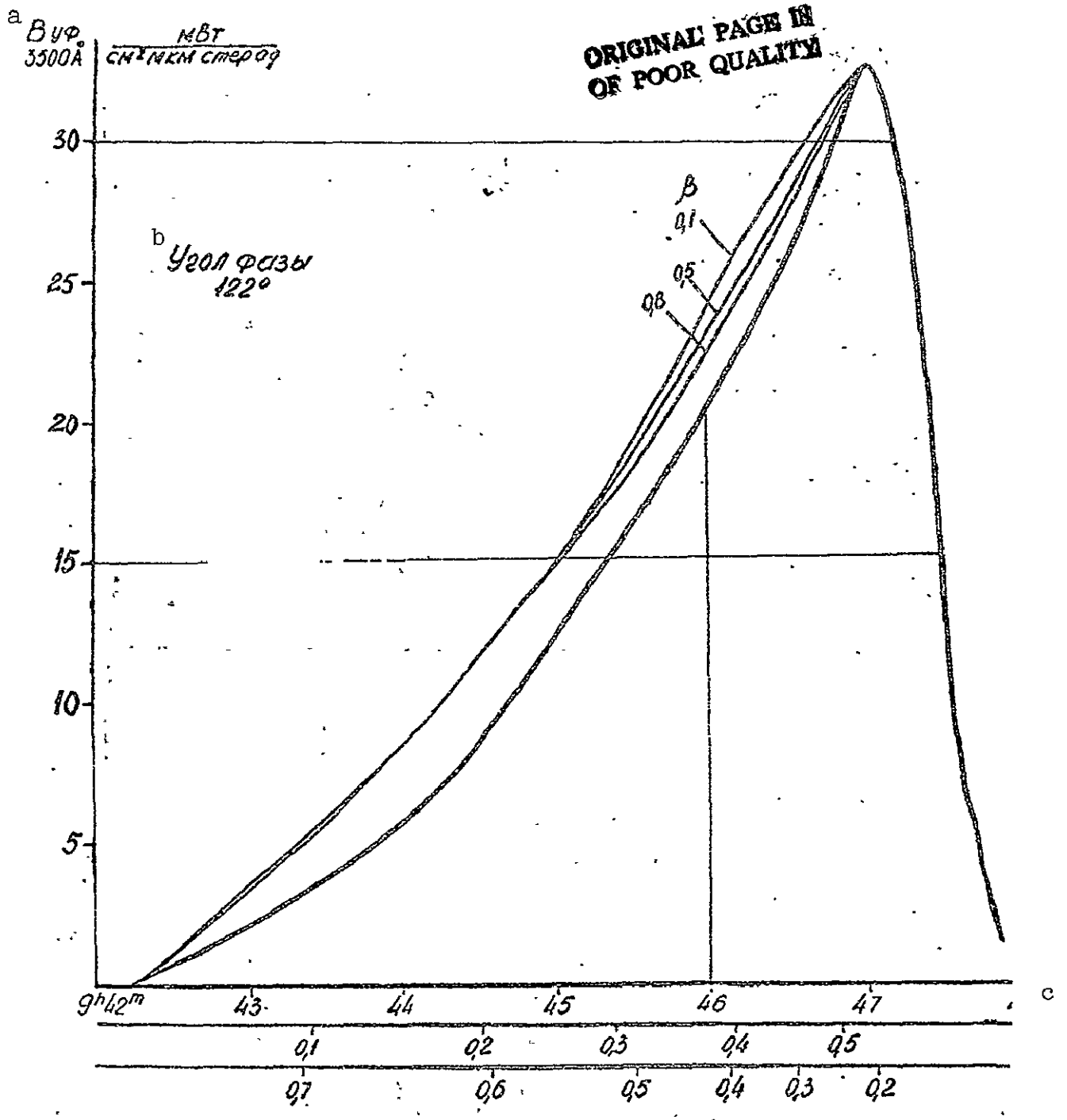


Fig. 12. Same as Fig. 11 for $\tau=0.6$ and $a=0.953$.

Key: [same as in Fig. 1].

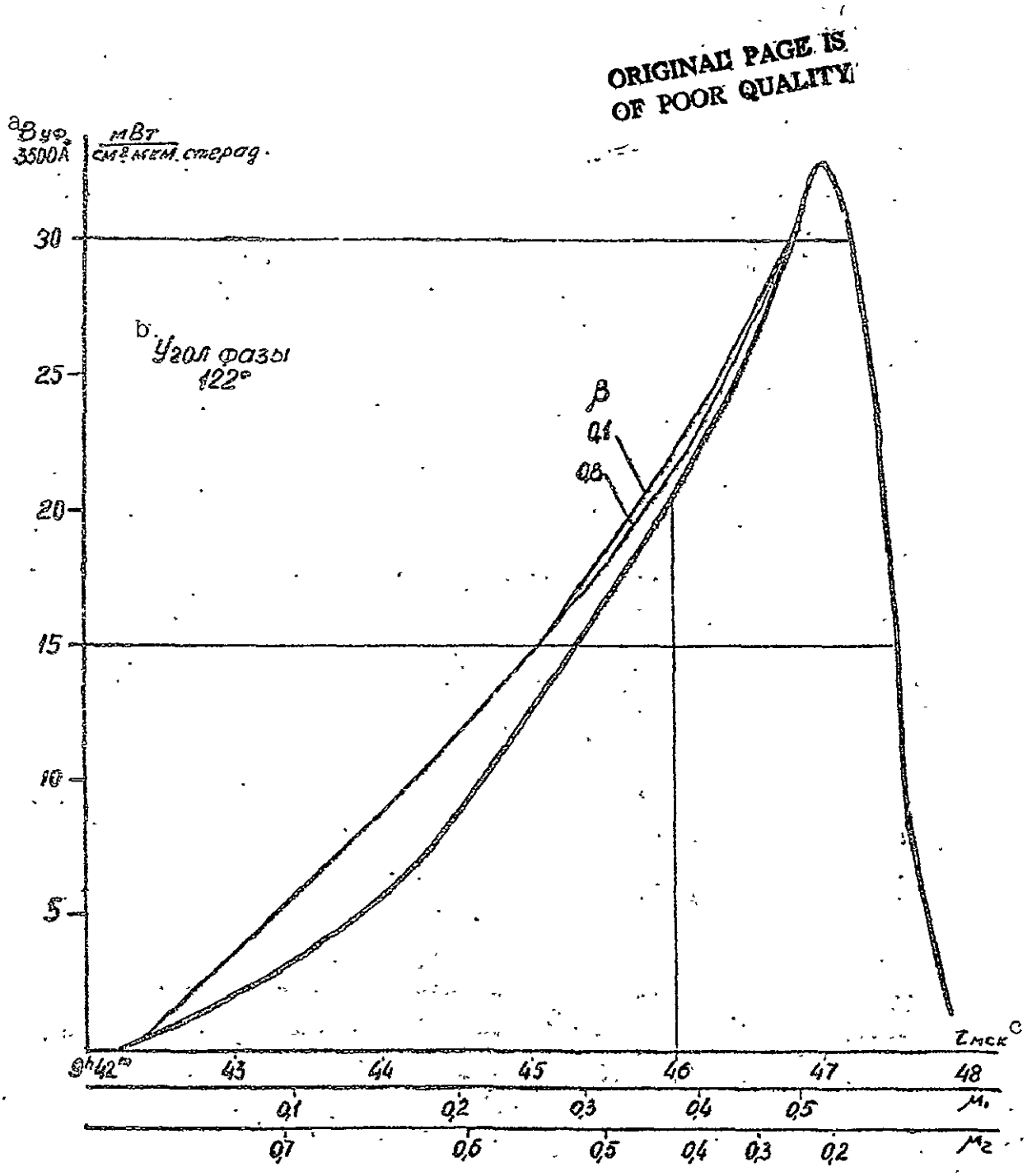


Fig. 13. Same as Fig. 11 for $\tau=0.9$ and $a=0.953$.

Key: [same as in Fig. 1].